Fully Physical Electro-Thermal CAD for Power FET Optimisation by Non Uniform Finger Spacing

A. J. Panks*, W. Batty+, S. David+, R. G. Johnson+ and C. M. Snowden*+,
*Filtronic plc., The Waterfront, Salts Mill Road, Saltaire, Shipley, W. Yorks, BD18 3TT, UK.
+Institute of Microwaves and Photonics, School of Electronic and Electrical Engineering, University of Leeds, Leeds LS2 9JT, UK.
Tel. +44 1274 231418, E-mail apanks@filct.com

Abstract

A fully physical electro-thermal model is described. It combines the fast, quasi-2-dimensional Leeds Physical Model of MESFETs and HEMTs, with the compact Leeds thermal impedance matrix model of time-dependent heatflow in complex 3-dimensional systems. The coupled electro-thermal model is applied to the design optimisation of multigate power FETs. In particular, the possibility of reducing temperature variation between gate fingers by non uniform spacing is examined. The implications for improved efficiency, and for possible reduction of thermal intermodulation distortion and improvement of reliability are discussed. The model is validated experimentally by comparison of simulated results against infrared thermal images of power FETs.

I. Introduction

Fully physical modelling offers the possibility of examining the effects on device performance of structure and layout, without the need to make expensive prototype fabrication and characterisation runs. This paper describes the application of a fully physical, coupled electro-thermal model of power FETs, in the optimisation of power FET design. Design optimisation in a multigate power FET is achieved by non uniform spacing of fingers. Simulated results are compared against experimentally obtained high resolution infrared images.

Typical power FET designs are based on uniform finger spacing. However, non uniform spacing offers a degree of design freedom to increase temperature uniformity and to reduce peak temperatures. Conventional designs typically show a temperature peak at the center of the multifinger device, with temperatures dropping to a minimum for the outermost fingers. As active device channels will all experience the same gate-source and drain-source voltages, V_{GS} and V_{DS}, this temperature variation means that drain currents, I_D, will vary from finger to finger, largely due to the impact on temperature dependent mobility of temperature variation between fingers. This could in turn lead to temperature dependent efficiency, distortion and reliability issues, which will be significant in devices such as power amplifiers for mobile communications.

II. The Leeds Physical Model

The Leeds Physical Model (LPM) [1]–[4] is a quasi-2D physical model of MESFETs and HEMTs including the effects of self-heating. The quasi-2D approximation is based on the observation, from full 2-dimensional simulations, that carrier transport is essentially 1-dimensional and driven by the component of electric field along the device channel. The LPM solves hydrodynamic equations obtained from moments of the Boltzmann equation. It consists of continuity, momentum and energy conservation, and heat diffusion equations.

The LPM solves Poisson and Schrodinger equations self-consistently in the direction normal to the heterointerface, to describe charge control, Fig. 1. The charge control information is calculated prior to calculation of in-plane transport and is stored as a look-up table. The quasi-2D model includes a full description of the device cross-section, by describing charge conservation in the vicinity of the device channel via a series of Gaussian boxes, Fig 2. The Leeds Physical Model incorporates the effects of temperature on device performance by use of a temperature dependent low field mobility. Velocity-field characteristics are obtained from Monte Carlo simulations and stored as a simple parameterisation. The LPM provides a physical large signal description of device performance. It forms the core of the coupled electro-thermal solution presented in this paper.

III. The Leeds Thermal Impedance Matrix Model

The Leeds thermal impedance matrix model [5]–[8] solves the non linear time-dependent heat diffusion equation,

$$\nabla . [\kappa(T)\nabla T] + g = \rho C \frac{\partial T}{\partial t}, \quad (1)$$

where T is temperature, t is time, $\kappa(T)$ is temperature dependent thermal conductivity, $g(x, y, z, t)$ is rate of heat generation, ρ is density and C is specific heat. It solves this equation fully analytically in complex volumes

using the Kirchhoff transformation [9] and a subsequent time variable transformation [10], [11] to fully linearise the equation [7]. The thermal impedance matrix approach then reduces to construction of global heat flow functions, for power dissipating and temperature sensitive elements in semiconductor integrated circuits, as

$$\overline{\Delta\theta_i} = \sum_j R_{TH_{ij}}(s)\overline{P_j} \tag{2}$$

where $\overline{\Delta\theta_i}$ is the Laplace transformed temperature rise of element i above its initial temperature, $R_{TH_{ij}}(s)$ is the thermal impedance matrix in Laplace s-space and the $\overline{P_j}$ are the transformed time-dependent fluxes due to power dissipation in elements, $j = 1, ..., i, ...M$.

Laplace inverting the impedance matrix equation, Eq (2), either analytically or numerically, the temperature rise of element i at time $\tau = m\delta\tau$, $\Delta\theta_i^{(m)}$, is obtained as a function of the time step power dissipations $P_j^{(n)}$. Writing $\Delta\theta_i^{(m)} = \Delta\theta_i^{(m)}(P_i^{(m)})$ from the electrical model then gives,

$$\Delta\theta_i^{(m)}(P_i^{(m)}) = \sum_n \sum_j \left[u(m-n+1)R_{TH_{ij}}((m-n+1)\delta\tau) - u(m-n)R_{TH_{ij}}((m-n)\delta\tau)\right] P_j^{(n)}, \tag{3}$$

where $u(\tau)$ is the unit step function. These coupled electro-thermal equations are solved self-consistently.

For the generic thermal subvolume of Fig. 3, the corresponding form of the thermal impedance matrix is,

$$R_{TH_{ij}}(s) = \frac{1}{\kappa_S LW} \sum_{mn} \frac{I^i_{mn} I^j_{mn}}{I^i_{00}} \frac{-4}{(1+\delta_{m0})(1+\delta_{n0})} \frac{1}{\gamma^2_{mn}} \left[\begin{array}{c} \frac{\sinh\gamma_{mn}z_{i2} - \sinh\gamma_{mn}z_{i1}}{\gamma_{mn}(z_{i2}-z_{i1})} \times \\ \frac{[\cosh\gamma_{mn}(D-z_{i1}) - \cosh\gamma_{mn}(D-z_{i2})]}{\cosh\gamma_{mn}D} \\ +1 - \frac{\sinh\gamma_{mn}(z_{i2}-z_{i1})}{\gamma_{mn}(z_{i2}-z_{i1})} \end{array} \right], \tag{4}$$

$$\gamma^2_{mn} = \left(\frac{m\pi}{L}\right)^2 + \left(\frac{n\pi}{W}\right)^2 + \frac{s}{k_S}, \quad I^i_{mn} = \iint_{D_i} \cos\left(\frac{m\pi x}{L}\right) \cos\left(\frac{n\pi y}{W}\right) dxdy, \quad m, n = 0, 1, 2, ..., \tag{5}$$

where, z_{i1}, z_{i2} are the z-coordinates of the planes bounding heat dissipating volume, i, in the z-direction and D_i is the corresponding $x - y$ cross-section. κ_S is thermal conductivity and k_S is diffusivity, $\kappa_S/\rho C$, both at Kirchhoff transformation temperature, T_S. δ_{mn} is the Kronecker delta function.

This expression provides the thermal solution in the form of generalised multiport thermal Z-parameters describing a thermal N-port, Fig. 3 (inset) [8]. This approach readily generalises to treat structural detail such as surface metallisation, vias and airbridges [5]–[8].

IV. Non Uniform Finger Spacing

Simulations based on numerical solution of the 2-dimensional heat diffusion equation along the active device channel length, show that non uniform finger spacing can reduce peak temperatures and can also reduce temperature variation between fingers. 2-dimensional numerical simulations have been compared against the fully analytical 3-dimensional thermal impedance matrix simulations outlined above. Areal temperature distributions have been plotted, as in Fig. 4. Use of the 3-dimensional thermal impedance matrix model in a non linear root finding algorithm, to search parameter space for the optimum separation of finger spacings, is described below.

As a first step towards device layout optimisation, the thermal resistance matrix is optimised for a bare GaAs die by variation of finger spacing. Optimal design is chosen to be that with the most uniform distribution of peak temperatures in active device channels. Fig. 5 illustrates three configurations used for comparison. A little thought makes apparent that on a die with adiabatic sidewall boundary conditions, symmetrically placed fingers with finger spacing of exactly L/N, where L is the die width and N is the number of fingers, will give exactly uniform temperatures at device channels. This configuration is shown in Fig. 5 (a). However, this requires a separation of edge fingers and die edges, of just $L/2N$, which will typically be too small to allow dicing of a semiconductor wafer. The same uniform finger spacing, but allowing for a significant border around the die fingers, is illustrated in Fig. 5 (b). However, this configuration will now produce non uniform temperature distribution across die fingers. Finally, Fig. 5 (c) illustrates the proposed optimisation of device design, by non uniform finger spacing, within the prescribed border, to achieve uniformity of device temperatures.

A. Non linear optimisation

Non linear optimisation is achieved by employing the thermal resistance matrix in a multidimensional direction set (Powell's) method and in a simulated annealing approach based on a modification of the downhill simplex method [12].With $\Delta\theta_i$ the temperature rise in active channel, i, due to power dissipations, P_j, in active channels, $j = 1, ..., i, ..., N$, and putting $P_j = P$ for all j, the mean temperature rise, $\overline{\Delta\theta}$, is given as,

$$\Delta\theta_i = \sum_j R_{TH_{ij}} P_j, \quad \overline{\Delta\theta} = \frac{P}{N} \sum_{ij} R_{TH_{ij}}. \tag{6}$$

Optimisation is then chosen to correspond to minimisation of the function,

$$\sigma = \sqrt{\frac{1}{N}\sum_i \left(\Delta\theta_i - \overline{\Delta\theta}\right)^2}. \tag{7}$$

Fixing the outer fingers at the required border, and using symmetry for a 10-finger device, this is a non linear minimisation problem for the function $\sigma(\Delta x_1, \Delta x_2, \Delta x_3, \Delta x_4)$, with Δx_i the independent finger separations.

V. Simulated results

After optimisation of the thermal resistance matrix, coupled electro-thermal simulations were performed by combination with the Leeds Physical Model (LPM) of MESFETs and HEMTs [1]–[4]. Coupling the thermal resistance matrix to the LPM, the results of Figs. 6–8 were obtained. Fig. 6 illustrates the totally uniform temperature response obtained in the unrealistic case of completely optimal uniform finger spacing without a significant die border. Fig. 7 illustrates the conventional temperature profile obtained with uniform finger spacing on a successfully diced device. Finally, Fig. 8 illustrates the nearly uniform temperature profile obtained with non uniform finger spacing as determined by non linear optimisation. In contrast to the intuitive monotonic decrease of finger spacing suggested in Fig. 5 (c), the optimised result groups fingers in pairs.

VI. Experimental Validation

For model validation, fully physical electro-thermal simulations of a 24 mm gate length power HEMT were compared against thermal images obtained with an Inframetrics ThermaCam, Figure 4. Agreement was good.

VII. Conclusions

A fully physical, coupled electro-thermal model of MESFETs and HEMTs has been described. This model has been used in the optimisation of FET design by non uniform finger spacing. The model has been validated experimentally by high resolution thermal imaging.

VIII. Acknowledgements

A. J. Panks, S. David and C. M. Snowden acknowledge financial support by the EPSRC. W. Batty and C. M. Snowden acknowledge support by the U.S. Army Research Office through Clemson University as part of a Multidisciplinary Research Initiative on Quasi-Optics, agreement Number DAAG55-97-K-0132. The authors are grateful to Filtronic plc for supplying FETs for this work.

References

[1] C. M. Snowden and R. R. Pantoja, 'Quasi-two-dimensional MESFET simulations for CAD,' *IEEE Trans. Electron Dev.*, vol. 36, pp. 1564–1574, 1989.

[2] C. G. Morton, J. S. Atherton, C. M. Snowden, R. D. Pollard and M. J. Howes, 'A large-signal physical HEMT model,' *IEEE MTT-S Internat. Microwave Symp. Dig.*, pp. 1759–1762, 1996.

[3] R. G. Johnson, C. M. Snowden and R. D. Pollard, 'A physics-based electro-thermal model for microwave and millimetre wave HEMTs,' *IEEE MTT-S Internat. Microwave Symp. Dig.*, vol. 3, Paper TH3E-6, pp. 1485–1488, 1997.

[4] L. Albasha, R. G. Johnson, C. M. Snowden and R. D. Pollard, 'An investigation of breakdown in power HEMTs and MESFETs utilising an advanced temperature-dependent physical model,' *Proc. IEEE 24th Internat. Symp. Compound Semiconductors*, pp. 471–474, San Diego, 1997.

[5] W. Batty, A. J. Panks, R. G. Johnson and C. M. Snowden, 'Electro-thermal modelling and measurement for spatial power combining at millimeter wavelengths,' *IEEE Trans. Microwave Theory Tech.*, vol. 47, no. 12, pp. 2574–2585, 1999.

[6] W. Batty, A. J. Panks, R. G. Johnson and C. M. Snowden, 'Electro-thermal modelling of monolithic and hybrid microwave and millimeter wave IC's,' *VLSI Design*, vol. 10, no. 4, pp. 355–389, 2000.

[7] W. Batty and C. M. Snowden, 'Electro-thermal device and circuit simulation with thermal non linearity due to temperature dependent diffusivity,' *Electron. Lett.*, vol. 36, no. 23, pp. 1966–1968, 2000.

[8] W. Batty, C. E. Christoffersen, S. David, A. J. Panks, R. G. Johnson, C. M. Snowden and M. B. Steer, 'Fully physical time-dependent compact thermal modelling of complex non linear 3-dimensional systems for device and circuit level electro-thermal CAD,' *Proc. 17th Annual IEEE Semiconductor Thermal Measurement and Management Symp. (SemiTherm XVII)*, San Jose, pp. 71–84, March 2001.

[9] W. B. Joyce, 'Thermal resistance of heat sinks with temperature-dependent conductivity,' *Solid-State Electronics*, vol. 18, pp. 321–322, 1975.

[10] V. Kadambi and B. Dorri, 'Solution of thermal problems with nonlinear material properties by the boundary integral method,' in C. A. Brebbia, ed., BETECH 85 (Springer, Berlin, 1985).

[11] L. C. Wrobel and C. A. Brebbia, 'The dual reciprocity boundary element formulation for nonlinear diffusion problems,' *Comp. Meth. Appl. Mech. Eng.*, vol. 65, pp. 147–164, 1987.

[12] W. H. Press, S. A. Teukolsky, W. T. Vetterling and B. P. Flannery, 'Numerical Recipes in C, 2nd Edition,' Cambridge University Press, 1992, (Chapter 10).

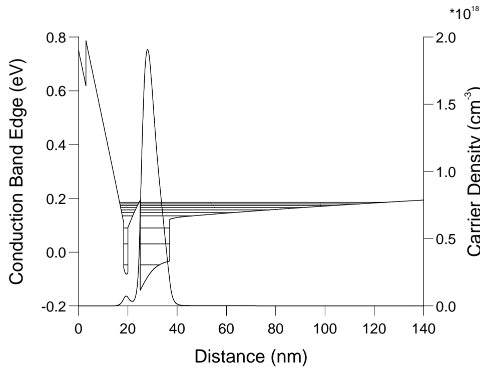

Fig. 1. Self-consistent Schrodinger-Poisson solution from the LPM for HEMT band-edge profile, subband structure, and carrier density normal to the heterointerface.

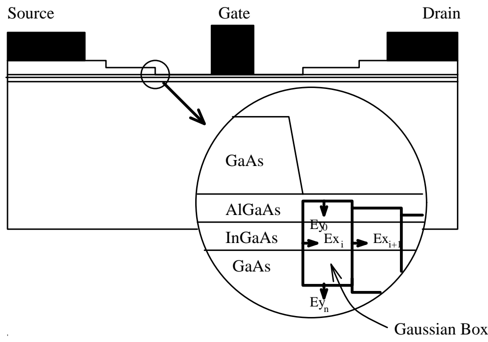

Fig. 2. FET cross-section and layer structure illustrating Gaussian boxes used in the LPM to model the 2-d profile.

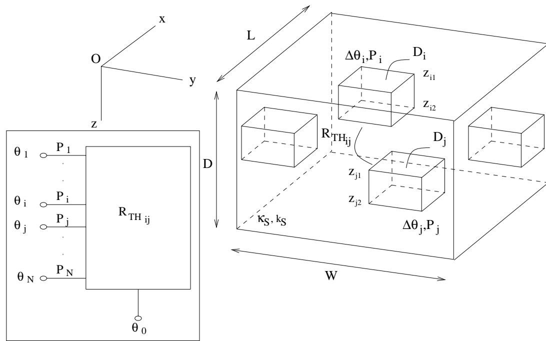

Fig. 3. Thermal subvolume with arbitrary distribution of power dissipating volumes, for construction of thermal impedance matrix, $R_{TH_{ij}}(s)$. Inset: corresponding thermal N-port.

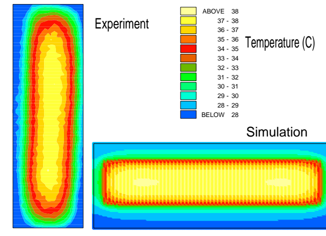

Fig. 4. Measurement and electro-thermal simulation of surface temperature in a 60-finger power HEMT. Bias (V_{DS}, V_{GS}) = (8 V, -1.5 V) and power dissipation is 3.2 W.

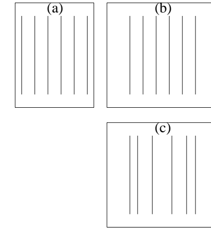

Fig. 5. Schematic finger spacings of a multi-gate FET: (a) optimal uniform finger spacing (b) non optimal uniform finger spacing (c) optimal non uniform finger spacing.

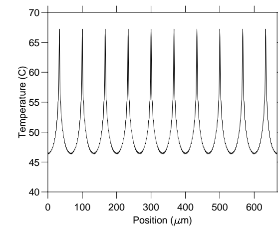

Fig. 6. Coupled electro-thermal simulation of surface temperature profile for (a) optimal uniform finger spacing.

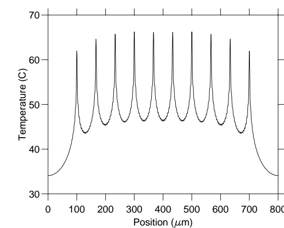

Fig. 7. Coupled electro-thermal simulation of surface temperature profile for (b) non optimal uniform finger spacing.

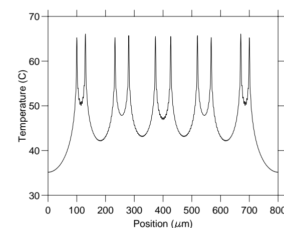

Fig. 8. Coupled electro-thermal simulation of surface temperature profile for (c) optimal non uniform finger spacing.